LBL-14160
Revised

CONF-821106--11 Rev.

Lawrence Berkeley Laboratory
UNIVERSITY OF CALIFORNIA

EARTH SCIENCES DIVISION

To be presented at the American Institute of Chemical Engineers National Heat Transfer Conference, Los Angeles, CA, November 8-12, 1982; and to be published in the proceedings

ANALYSIS OF FIELD-PERFORMANCE DATA ON SHELL-AND-TUBE HEAT EXCHANGERS IN GEOTHERMAL SERVICE

P.T. Doyle and L.F. Silvester

September 1982

MASTER

DISTRIBUTION OF THIS DOCUMENT IS UNLIMITED

Prepared for the U.S. Department of Energy under Contract DE-AC03-76SF00098

LEGAL NOTICE

This book was prepared as an account of work sponsored by an agency of the United States Government. Neither the United States Government nor any agency thereof, nor any of their employees, makes any warranty, express or implied, or assumes any legal liability or responsibility for the accuracy, completeness, or usefulness of any information, apparatus, product, or process disclosed, or represents that its use would not infringe privately owned rights. Reference herein to any specific commercial product, process, or service by trade name, trademark, manufacturer, or otherwise, does not necessarily constitute or imply its endorsement, recommendation, or favoring by the United States Government or any agency thereof. The views and opinions of authors expressed herein do not necessarily state or reflect those of the United States Government or any agency thereof.

Lawrence Berkeley Laboratory is an equal opportunity employer.

DISCLAIMER

This report was prepared as an account of work sponsored by an agency of the United States Government. Neither the United States Government nor any agency Thereof, nor any of their employees, makes any warranty, express or implied, or assumes any legal liability or responsibility for the accuracy, completeness, or usefulness of any information, apparatus, product, or process disclosed, or represents that its use would not infringe privately owned rights. Reference herein to any specific commercial product, process, or service by trade name, trademark, manufacturer, or otherwise does not necessarily constitute or imply its endorsement, recommendation, or favoring by the United States Government or any agency thereof. The views and opinions of authors expressed herein do not necessarily state or reflect those of the United States Government or any agency thereof.

DISCLAIMER

Portions of this document may be illegible in electronic image products. Images are produced from the best available original document.

LBL-14160 Revised

LBL--14160-Rev

DE83 001564

Analysis of Field Performance Data on Shell-and-Tube Heat Exchangers in Geothermal Service

P. T. Doyle* and L. F. Silvester+

ABSTRACT

Problems encountered in supercritical heat transfer calculations are discussed. Data evaluation models and results for primary heaters and condenser are presented. Results cover predicated areas, overall heat transfer coefficients, shell side film coefficients, mean temperature differences, pinch points, shell side pressure drops, and condensing coefficients. Test results are for isobutane and mixtures of isobutane/isopentane.

DISCLAIMER

This report was prepared as an account of work sponsored by an agency of the United States Government. Neither the United States Government nor any agency thereof, nor any of their employees, makes any warranty, express or implied, or assumes any legal liability or responsibility for the accuracy, completeness, or usefulness of any information, apparatus, product, or process disclosed, or represents that its use would not infringe privately owned rights. Reference herein to any specific commercial product, process, or service by trade name, trademark, manufacturer, or otherwise, does not necessarily constitute or imply its endorsement, recommendation, or favoring by the United States Government or any agency thereof. The views and opinions of authors expressed herein do not necessarily state or reflect those of the United States Government or any agency thereof.

*Heat Transfer Consultants, Inc.
1714 Linda Drive
P. O. Box 23525
Pleasant Hill, California 94523

+Earth Sciences Division
Lawrence Berkeley Laboratory
University of California
Berkeley, California 94720

NOTICE
PORTIONS OF THIS REPORT ARE ILLEGIBLE. It has been reproduced from the best available copy to permit the broadest possible availability.

This work was supported by the Assistant Secretary for Conservation and Renewable Energy, Office of Renewable Technology, Division of Geothermal and Hydropower Technologies of the U.S. Department of Energy under Contract No.DE-AC03-76SF00098.

DISTRIBUTION OF THIS DOCUMENT IS UNLIMITED

Introduction

Many geothermal binary cycles call for shell-and-tube heat exchangers operating with supercritical hydrocarbon mixtures. The supercritical region of interest lies in the near critical region and consequently is marked by high nonlinearity in the thermophysical properties. Because of this, at issue is what special calculational techniques and/or modifications to existing heat transfer correlations are necessary to predict the performance of such exchangers. The Supercritical Heat Exchange Field Test was run to provide data on the problem. The results of the data analysis are reported herein. Heat transfer measurements cover isobutane, 90/10 (mole %) isobutane/isopentane, and 80/20 isobutane/isopentane mixtures. Details of the experiment are reported elsewhere.[1, 2]

Analysis of Primary Heaters

The heat exchanger train consisted of six series connected exchangers (B-1 through B-6 in Figure 1) in counterflow with hydrocarbon in the shells and brine in the tubes. Table 1 lists the salient specifications.

In analyzing the data we employed the relationships,

$$Q = U*A*\Delta t_{mean} \tag{1}$$

$$\frac{1}{U} = \frac{1}{h_{io}} + r_{tube} + r_{wall} + r_{shell} + \frac{1}{h_o} \tag{2}$$

The tube inside film coefficient, h_{io}, was computed from the Dittus-Boelter equation, r_{shell} was taken as zero because of the clean state of the shell side, inspection of the tubes coupled with analysis of the data led to r_{tube} being taken as zero, and finally, h_o was computed from

$$h_o = C_o \cdot h_{corr} \tag{3}$$

where C_o is a constant and h_{corr} is given by a Dittus-Boelter-type equation for the shell-side. The value of C_o (= 1.116) and the form of h_{corr} were established by plotting the Nusselt number for longflow (Figure 2) and crossflow (Figure 3) vs. Reynolds number for data on the commercial isobutane tests away from the critical region and a water-water calibration test run prior to the field tests. The plots indicated h_{corr} could best be described by a longflow-type equation; consequently, h_{corr} was given as,

$$Nu = .024\ Re^{0.8}\ Pr^{0.4} \tag{4}$$

The exchanger pressure drops were also analyzed in conjunction with the heat transfer analysis. The tube side pressure drop was broken into channel nozzle losses, tube entrance and exit losses, and tube friction losses. The shell side presure drop was broken into longflow, crossflow, baffle window, and nozzle losses. Each component of pressure loss was represented by standard forms.[2] In addition, the shell-side pressure drop was taken as

$$\Delta P = C_s \cdot \Delta P_{corr} \tag{5}$$

where C_s could be adjusted until $\Delta P = \Delta P_{measured}$

Figure 4 is a typical T-Q plot for a 80/20 test run. The shape of the hydrocarbon curve is a direct result of the change in the thermophysical properties (Figure 5) and their effect on the engineering parameters (Figure 6). To handle such nonlinear behavior, each exchanger was subdivided into zones of sufficiently small width that equation 1 could be applied throughout the zone based upon the terminal temperatures of the zone and thermophysical properties averaged over the zone. Two types of calculations were run with the zone analysis.

Method One:

For Method One the computed temperature-pressure profile for the entire heat exchanger train was forced to conform to the experimental profile. Each exchanger's entrance and exit state point was fixed at the measured values. The computed hydrocarbon pressure drop for each exchanger was made to conform to the experimental value by adjusting the C_s parameter. Since the entrance and exit pressure and temperature were fixed, so were the enthalpies; therefore the ΔH for each hydrocarbon zone was based upon the overall hydrocarbon ΔH and not a first law heat balance applied to each zone, albeit the brine side duty was used in equation 1.

A comparison of the predicated area and the known area is given in Table 2. Entries are the average of the individual values from the data scans for the cited test fluid.

The A_{dev} values are based upon the total exchanger area for B-1 through B-5 and B-6 respectively. The averaged individual exchanger areas are listed, plus their standard deviation, Std, and the percent deviation, % Dev, from the known exchanger area.

The values of A_{dev}, and the individual areas for B-1 through B-5 are in excellent agreement with experiment. The value of C_s varies little for the three test fluids and shows a positive deviation of 1 to 9%.

The results suggest that the heat transfer and pressure drop algorithms chosen for modeling the exchangers are adequate for design purposes provided the temperature-pressure profile is known and adequate fluid properties are employed. This conclusion is further reinforced by the excellent fit to the mixture data for correlations scaled against the "pure" data. The maximum area deviation is less than 4% (Figure 7).

The results for B-6 show a consistent -20% area deviation irrespective of the test fluid. The results are consistent with Tleimat[3] who showed a lack of enhancement for h_o in the near critical region spanned by B-6.

Tables 3 and 4 list the other measured performance factors for B-1 through B-5 and B-6 respectively. Each entry is an averaged value of the data scans for the test cited. The listed values of U_m (m = measured) and $h_{o,m}$ were computed for each zone from

$$U_m = Q/A \, \Delta t_{mean} \tag{6}$$

$$\frac{1}{h_{o,m}} = \frac{1}{U_m} - r_{wall} - \frac{1}{h_{io}} \tag{7}$$

then averaged over the entire train.

The values of U_m for B-1 through B-5 vary from 429 to 261. The general trend of U_m is to lower values with increasing mole fraction of isopentane (for example, compare $h_{o,m}$ values for test runs 7, 21, and 31).

The values of U_m for B-6 vary from 538 to 295 and are larger than those for B-1 through B-5 because of the enhanced heat transfer in the region spanned by B-6. For B-6, the effect of fluid composition on U_m is harder to detect because of the greater uncertainty in the values of U_m.

Method Two:

The second method of prediction treats the entire train of heaters (B-1 through B-5) as one long heat exchanger. Only the temperature and pressure of the cold end are provided. The calculation proceeds from B-1 through B-5. Errors in the pressure drop prediction are accumulative as the pressure and temperature at the outlet of each zone is the inlet value for the next zone. For this calculational scheme, C_s is fixed at 1.0115 and a first law heat balance is forced on each zone. The C_s value was obtained as the average of the individual values for the data scans for the commercial isobutane tests run with C_o fixed at 1.116.

Rather than run all the data scans and report out averaged values, one data scan representative of each test run was selected for analysis. The resulting performance factors are compared in Table 5 to those obtained from the first calculational method. The A_{dev} values are for the total area of B-1 through B-5. The quantities subscripted with "m" are measured values from the first calculational method. The subscript 1 and 2 refer respectively to the first and second calculational methods, and the subscript "dev" is computed relative to the measured quantity.

We noted that with few exceptions U and U_m agree quite well, as do h_o and $h_{o,m}$, and P_{dev} is within acceptable limits. However, A_{dev} varies considerably. An interesting point is the consistently smaller computed pinch point ($P-P_{2t}$) versus the experimental value, $P-Pt_1$. This means the temperature-pressure profile as computed lies closer to the brine duty line than indicated by experiment. The result is a smaller LMTD for many zones and a concomitantly larger area.

The relationship is nicely demonstrated by the T-Q plot of Figure 8 for test run 21 (nominal 90/10 test fluid). The dotted line is the experimental hydrocarbon curve (method one calculation), the solid line the computed hydrocarbon curve (method two calculation). Both curves are qualitatively identical. Note however, the rapid increase in the computed temperature and the severe transition after the pinch point. There appears to be a critical pinch point of around 8 to 10°F, below which the calculated pinch point and the area deviate strongly from experiment.

Figures 9 and 10 illustrate the amount of area or pressure drop to heat the hydrocarbon at supercritical conditions. Figure 9 is a temperature versus area profile for test run 25A. The hydrocarbon temperature rises 148°F (125 to 273°F) in the first half of the train, but only 40°F (273 to 313°F) in the last half. Figure 10 is a pressure versus temperature profile for test run 25A. The hydrocarbon pressure drops 33 psia (675 to 642 psia) in the first half of the train, and 43 psia (642 to 599 psia) in the last half.

Data Analysis Condenser:

Whereas the intent of the primary heater data analysis was to validate the heater performance, for the condenser the intent was to report "measured" quantities such as overall heat transfer coefficients, shell side film coefficients, Reynolds numbers, etc. These measured quantities could then be used

as a benchmark for larger or more complicated condenser designs. We attempted to maintain a simple approach whose results would have the widest applicability. Consequently, we chose "conventional" models and dispensed with any stepwise calculations across the tube bundle. Table 6 lists the condenser specifications.

A modified form of the basic heat transfer equation was used for the condenser:

$$Q_{cond} = U_{cond} A_{cond} MTD \tag{8}$$

where Q_{cond}, U_{cond}, and A_{cond} have their usual meaning and MTD is the mean temperature difference computed as,

$$MTD = F * LMTD \tag{9}$$

where LMTD is the log-mean-temperature difference defined for the condenser as

$$T_a = T_{vap} - T_{cw,out} \tag{10a}$$

$$T_b = T_{liq} - T_{cw,in} \tag{10b}$$

$$LMTD = (T_a - T_b)/\ell n\ (T_a/T_b) \tag{10c}$$

and F is a correction factor for non-isothermal conditions defined as

$$F = a/N_{tp} * \ell n(1 + \ell n(1-b/r)) \tag{11}$$

where

$$N_{tp} = 1 \text{ (number of tube passes)} \tag{11a}$$

$$r = (T_{vapor} - T_{liq})/(T_{cw,out} - T_{cw,in}) \tag{11b}$$

$$p = (T_{cw,out} - T_{cw,in})/(T_{vapor} - T_{cw,in}) \tag{11c}$$

$$b = r * p \tag{11d}$$

$$a = \ell n(1-p)/(1-b))/(r-1) \tag{11e}$$

The overall heat transfer coefficient was treated as a series of connected thermal resistances, i.e.,

$$\frac{1}{U_{cond}} = \frac{1}{h_{io}} + r_{tube} + r_{wall} + r_{shell} + \frac{1}{h_o} \tag{12}$$

Because we are interested in measured quantities, we wrote,

$$U_m = Q_{cond}/(A_{cond}MTD) \tag{13}$$

$$h_{o,m} = \frac{1}{\frac{1}{U_m} - r_{tube} - r_{wall} - r_{shell} - \frac{1}{h_{io}}} \tag{14}$$

The last three terms in equation 14 were computed from correlations which are functions of the thermophysical fluid properties and geometry factors. As with the primary heaters, the tube side film coefficient was computed from the Dittus-Boelter equation. The r_{shell} was taken at zero, and r_{tube} was determined from the data using a differential resistance analysis. Its variation with time is shown in Figure 11. Details of the calculation are given elsewhere.[2]

Finally a U_{clean} was completed from

$$U_{clean} = \frac{1}{\frac{1}{U_m} - r_{tube}} \tag{15}$$

The above equations assume wet tube wall conditions. The wet tube wall model was adopted because in all test runs the cooling water exit temperature was well below the hydrocarbon dew point temperature for the set condenser pressure. The condensing mechanism is therefore liquid on the tube wall in contact with vapor. Consequently, the dew point temperature is used in the model rather than the temperature of the incoming superheated vapor.

Each data scan was analyzed using the basic equations and the appropriate fouling resistance. Table 7 lists the performance factors for one selected data scan from each test run. Figure 12 is a plot of U_m and U_{clean} for the full bundle test runs of Table 7 against the test run number. Figure 13 is a plot of $h_{o,m}$ for the same test runs against the test run number.

From Figure 12 we see that U_m and U_{clean} decrease with increasing isopentane composition. These results are in qualitative argument with experimental data on single tube condensation.[4] The implication is that more surface area would be needed for a mixture than for pure isobutane running at

the same condenser pressure as the mixture. However, we note from Table 7 that the performance of commercial isobutane and nominal 80/20 mixture can be comparable for similar conditions, and in some cases the mixtures perform better. The other factor is the mixtures' higher temperature gradient for condensation for the same condenser pressure which apparently offsets the lower value of the film coefficient.

Figure 14 is a plot of Nu versus Rey_c for the results of Table 7. The left hand section is for laminar conditions; it is then followed by a transition region and a turbulent region where the film coefficient increases sharply. Most of the test data falls in the transition region with the half bundle tests in the turbulent region and at conditions more likely chosen for a commercial application.

Summary and Conclusions:

The test data for the primary heaters and condenser covering an area of commercial interest was analyzed using models common to the heat transfer industry. Analysis of the primary heater data yielded area predictions, overall heat transfer coefficients, shell side film coefficients, mean temperature differences, exchanger pinch points, and shell side pressure drop predictions. We found that:

1. Heat transfer and pressure drop correlations applicable in the liquid region (non-critical region) that yield state-of-the-art accuracy can be used as a basis for a stepwise performance calculation of a supercritical binary heat exchanger train.

2. Thermodynamic and transport property algorithms are an integral part of the performance correlation. The use of other property data will produce results different from those found in this investigation.

3. When the heat transfer and pressure drop correlations employed were empirically adjusted, though the standard forms were not modified, to give a high degree of accuracy for liquids well removed from the critical region, the correlations could then be used, unadjusted, for performance calculations of the experimental data from the liquid region through the near critical region.

4. When the hydrocarbon temperature-pressure profile along the exchanger train is known (in our case measured), the area calculated from the correlations agreed generally within 2% of the overall train area with predicted individual exchanger areas varying from -0.3 to 5.2% from the known values.

5. When the hydrocarbon temperature-pressure profile along the exchanger train was calculated (as in the case of designing an exchanger train) significantly greater error in the calculated area resulted. Experimental temperature pinch points ranged from 2.5 to 13.7°F with most values between 8 to 9°F. The P-H-T correlation generally predicted pinch points smaller than the experimental values resulting in overprediction of the required area. The overall train area calculated for commercial isobutane and nominal 80/20 isobutane/isopentane averaged 11% higher than the actual area. The calculated areas for nominal 90/10 isobutane/isopentane were much worse, averaging 70% higher.

6. For the 80/20 mixtures, when the operating pinch point was 10°F or greater, the calculated area was less than 12% larger than the known area. In general, for pinch points less than 10°F, the calculated areas deviated from 10 to 600%. Based upon our calculational methods, an increase in the operating temperature pinch appears necessary to reduce errors in the area to acceptable levels, particularly for the 90/10 mixture.

7. Additional experimental work on the thermodynamic properties in the near-critical region appears necessary to improve the accuracy of performance predictions for 90/10 mixtures, and for temperature pinch points of 10°F or less.

8. For the hot exchanger, the correlations consistently underpredicted the area by approximately 20%. The results are consistent with other investigators[3] that concluded the increased heat transfer effect in the near critical region is less than predicted by standard equations. Errors in the predicted area represented about 4% of the overall train area and appear not to introduce unacceptable errors for design of industrial heat exchanger trains spanning the temperature interval explored in this investigation. However, investigation of heat transfer in the near critical region is of interest and should be pursued and more fully understood.

9. Fouling of the brine or hydrocarbon was not measurable throughout the duration of the tests.

10. The overall heat transfer coefficients (Btu/hr-ft^2-°F) varied from 390 to 425 for commercial isobutane, 395 to 326 for the nominal 90/10 mixture, and from 351 to 402 for the nominal 80/20 mixture for the test conditions encountered.

Analysis of the condenser data yielded overall heat transfer coefficients, shell side film coefficients, mean temperature differences, and tube side fouling resistance as a function of time. We found that:

1. The relationship between time and fouling of the cooling water side as determined by measurements outlined in this investigation was necessary for obtaining the hydrocarbon condensing coefficients.

2. Assuming a wet tube wall for calculation of the mean temperature difference, and including the desuperheating duty in the total condensing heat load were applicable for the test conditions encountered.

3. The overall condensation coefficients for isobutane, 90/10 and 80/20 mixtures show a slight decrease with increasing isopentane content in agreement with earlier work.[4] The condensing coefficients (Btu/hr-ft^2-°F) for the full bundle tests were 190 to 240 for overall condensate Reynolds numbers of 600 to 2000. The half bundle tests increased the Reynolds number to 3700 to 4900 yielding condensing coefficients of 300 to 380.

4. The data further confirms the departure from Nusselt type condensation as higher tube loadings are achieved. For all the data taken, the condensing coefficient was essentially constant until Reynolds numbers of about 3700 were reached where the coefficient increased by 50%. No data was taken in the range of Reynolds number from 2200 to 3700; therefore the actual departure point was not determined.

Acknowledgments:

The authors thank R. Fulton and W. Pope of LBL for timely comments, Margaret Baker for preparation of the manuscript. This work was done under DOE Contract DE-AC03-76SF00098.

Notation:

A	surface area of tubes
h_{io}	inside heat transfer coefficient referred to outside surface area
h_o	outside heat transfer coefficient

LMTD	log-mean-temperature-difference
Nu	Nusselt number
P	pressure
Pr	Prandtl number
Q	exchanger duty
Re	Reynolds number
r_{tube}	tube side thermal resistance
r_{wall}	tube wall thermal resistance
r_{shell}	shell side thermal resistance
t_{mean}	mean temperature difference
U	overall heat transfer coefficient

Literature Cited:

1. L.F. Silvester, L.O. Beaulaurier, K.F. Mirk, and R.L. Fulton, "Supercritical Heat Exchange Field Test (SHEFT), I. Field Performance Data on Shell-and-Tube Heat Exchangers in Geothermal Service", LBL-12850, Lawrence Berkeley Laboratory, University of California, Berkeley, June 1981.

2. L.F. Silvester and P.T. Doyle, "Analysis of Field Performance Data on Shell-and-Tube Heat Exchangers in Geothermal Service", LBL-14160, Lawrence Berkeley Laboratory, University of California, Berkeley, March 1982.

3. B.W. Tleimat, A.D.K. Laird, I.C. Hsu, and H. Rie, "Baseline Data on Film Coefficient for Heating Isobutane Inside a Tube at 4.14 MPa (600 psia)," LBL-9720, Lawrence Berkeley Laboratory, Berkeley, California, April 1979.

4. B.W. Tleimat, H. Rie, A.D.K. Laird, and S. Zhao, "Condensation Film Coefficients for Mixtures of Isobutane and Isopentane", LBL-11025, Lawrence Berkeley Laboratory, Berkeley, California, May 1980.

Table 1

Primary heat exchanger details

No. of tubes per exchanger: 62
No. of passes: 1 shell side, 1 tube side
Tube length: 24 ft
Tube size: 3/4 in O.D., 16 BWG.
Tube Material: carbon steel (SA-214)
Tube pitch: 15/16 in., triangular array
Shell I.D.: 8.625
Baffle spacing: 12 in.
Baffle cut: horizontal cut segmental baffles, 13/16 in. from center line
Area per exchanger: 292 ft^2
Number of exchangers: 6
Nominal dia. shell side nozzles: 6 in.
Nominal dia. tube side nozzles: 3 in.
TEMA type E shell

Exchangers: B-1 thru B-5
Flow orientation: 30°
Baffle cut: 13/16 in. from center line
Cross flow area: 20.3 sq. in.
Net window area: 11.8 sq. in

Exchanger: B-6
Flow orientation: 60°
Vertical cut double segmental baffles
Center baffle cut: 2-11/32 in. from center line
Outer baffles cut: 1-13/32 in. from center line
Crossflow area: 20.3 sq. in.
Outer net window area: 10/6 sq. in.
Inner net window area: 9.9 sq. in.

Table 2

Exchanger Area form Method One Septwise Calculation

Commercial Isobutane

A_{dev} = 0.66 ± 1.51% C_s = 1.011 ± 0.052

Exchanger	A_{cal} (ft^2)	Std (ft^2)	% Dev
B-1	297.8	± 5.81	1.9
B-2	307.4	± 9.84	5.2
B-3	285.6	± 7.4	-2.3
B-4	283.9	± 9.5	-2.8
B-5	295.9	± 17.0	1.3

Nominal 90/10 Isobutane/Isopentane

A_{dev} = 1.38 ± 1.09% C_s = 1.088 ± 0.055

Exchanger	A_{cal} (ft^2)	Std (ft^2)	% Dev
B-1	290.3	± 4.3	-0.7
B-2	299.8	± 7.0	2.6
B-3	293.2	± 9.3	0.3
B-4	303.8	± 21.8	4.0
B-5	294.2	± 31.4	0.7

Nominal 80/20 Isobutane/Isopentane

A_{dev} = 2.32 ± 2.50% C_s = 1.032 ± 0.042

Exchanger	A_{cal} (ft^2)	Std (ft^2)	% Dev
B-1	282.1	± 1.5	-3.5
B-2	291.2	± 5.0	-0.3
B-3	282.7	± 13.2	-3.3
B-4	286.2	± 20.2	-2.0
B-5	284.8	± 25.0	-2.5

- - - - - - - - - - - - -

Exchanger B-6

Commercial Isobutane

A_{dev} = 22.4 ± 13.6% C_s = 1.016 ± 0.182

A_{cal} = 226.7 ± 39.7 (ft^2)

Nominal 90/10 Isobutane/Isopentane

A_{dev} = -19.4 ± 5.4% C_s = 1.196 ± 0.156

A_{cal} = 244.2 ± 15.9 (ft^2)

Nominal 80/20 Isobutane/Isopentane

A_{dev} = -15.9 ± 11.0% C_s = 1.184 ± 0.093

A_{cal} = 245.5 ± 32.1 (ft^2)

Table 3

Performance for B-1 through B-5 from Method One Calculation

Run #	$T_{Br,in}$ (°F)	$T_{Br,out}$ (°F)	m_{Br} (lbs/hr)	$T_{Hc,in}$ (psia)	$P_{Hc,in}$ (psia)	$T_{Hc,out}$ (°F)	$P_{Hc,out}$ (psia)	m_{HC} (lbs/hr)	Duty (Btu/hr) x10^{-6}	WTD (°F)	U_m	$h_{o,m}$	P-Pt (°F)
--- Commercial Isobutane ---													
1	309.9	205.2	93200	140.6	666.8	292.0	620.4	74513	9.92	17.4	391	670	8.3
2	327.1	218.0	93365	131.5	653.9	309.7	616.3	60547	10.4	18.7	379	628	8.1
5	307.7	207.9	102357	152.1	675.8	290.4	619.9	83088	10.4	16.7	425	746	8.5
6	303.3	201.9	99136	152.2	651.8	285.3	593.0	86505	10.2	16.8	415	730	9.1
7	319.7	213.0	101133	142.8	639.4	295.8	593.2	71180	11.0	17.8	424	739	8.2
8	342.8	239.3	101006	138.1	635.7	339.2	585.9	53484	10.7	19.8	372	580	2.6
10	305.8	206.3	101684	157.0	656.3	286.4	596.0	86811	10.3	16.4	429	761	9.0
11	300.0	205.5	95408	161.1	633.1	281.5	575.3	88175	9.2	15.5	403	711	8.5
12	321.6	212.7	95938	146.5	616.8	293.9	571.9	69052	10.7	17.9	407	708	8.0
13	296.3	201.0	64052	146.3	584.4	279.1	561.7	53366	6.2	16.6	261	432	6.6
15	301.7	207.3	97556	162.1	632.8	281.8	575.7	84258	9.4	15.7	408	715	8.6
--- 9/10 Isobutane/Isopentane ---													
18	316.7	202.4	93051	119.1	655.9	298.4	615.6	69858	10.8	19.6	379	607	8.5
19	334.9	220.0	80142	118.0	637.0	322.6	612.2	48672	9.4	19.5	330	529	8.1
20	305.6	191.9	98963	130.1	650.8	289.5	591.3	84485	11.4	20.0	391	660	10.7
21	345.5	202.7	44921	118.4	639.4	317.9	588.2	68725	13.9	24.1	393	663	11.3
22	340.6	204.3	70876	124.0	603.9	316.4	577.4	49535	9.9	21.0	322	537	8.8
23	306.0	193.4	100440	121.7	625.9	288.0	572.7	78711	11.5	19.9	394	662	9.1
24	343.6	218.0	98306	121.5	621.9	329.6	575.4	62899	12.6	22.4	386	630	10.5
25	341.3	219.4	75479	134.8	593.5	329.7	565.2	48090	9.4	19.8	326	530	8.9
--- 80/20 Isobutane/Isopentane ---													
25A	315.1	192.6	96328	125.6	675.1	302.0	615.5	90258	12.0	21.6	380	633	11.4
26	344.7	197.7	96656	122.6	684.3	315.8	622.1	88362	14.5	24.7	402	686	13.7
28	316.6	201.5	85599	126.9	654.3	304.7	614.8	72582	10.0	20.1	341	551	9.4
29	330.9	229.6	86270	130.0	634.5	316.6	608.2	53067	8.9	17.5	351	562	7.0
30	310.2	192.9	96560	134.8	656.2	296.2	592.8	93821	11.5	20.7	380	635	11.2
31	316.4	210.3	96514	133.0	635.0	302.5	591.3	75087	10.4	19.3	369	597	8.7
32	324.6	222.6	85921	129.5	612.1	307.1	584.9	55691	8.9	17.6	348	560	6.8
33	307.6	196.4	100502	140.7	636.9	293.5	569.7	96419	11.4	19.8	393	660	10.6
34	314.3	208.4	100389	129.2	615.6	298.3	568.6	77524	10.8	19.4	382	620	8.0
35	337.8	230.1	100746	123.3	602.5	324.1	565.6	57842	11.1	20.7	368	575	8.2
36	317.8	206.1	100603	135.2	675.4	304.8	619.8	85595	11.4	20.4	383	634	10.1

Table 4

Performance for B-6 from Method One Calculation

Run #	$T_{Br,in}$ (°F)	$T_{Br,out}$ (°F)	m_{Br} (lbs/hr)	$T_{Hc,in}$ (psia)	$P_{Hc,in}$ (psia)	$T_{Hc,out}$ (°F)	$P_{HC,out}$ (psia)	m_{Hc} (lbs/hr)	Duty (Btu/hr) x10^{-6}	WTD (°F)	U_m	$h_{o,m}$
--- Commercial Isobutane ---												
1	339.4	309.9	93200	292.0	620.4	314.5	603.0	74513	2.85	24.2	403	674
2	338.9	327.1	93365	309.7	616.3	329.2	600.8	60547	1.15	13.4	295	416
5	339.5	307.7	102357	290.4	619.9	311.0	599.5	83088	3.37	25.0	462	820
6	342.8	303.3	99136	285.3	593.0	307.6	570.6	86505	4.06	29.1	478	888
7	342.6	319.7	101133	295.8	593.2	325.9	572.2	71180	2.41	22.1	373	576
10	344.9	305.8	101684	286.4	596.0	311.5	572.6	86811	4.13	29.9	474	860
11	344.3	300.0	95408	281.5	575.3	307.4	552.1	85175	4.36	31.1	480	917
12	344.6	321.6	95938	293.9	571.9	328.7	549.9	69052	2.29	22.6	346	523
13	338.0	296.3	64052	279.1	561.7	310.1	551.8	53366	2.76	27.0	350	631
15	344.4	301.7	97556	281.8	575.7	309.3	552.2	84258	4.32	31.6	468	861
--- 90/10 Isobutane/Isopentane ---												
18	342.3	316.7	93051	298.4	615.6	322.7	599.7	69858	2.48	21.7	392	641
19	341.5	334.9	80142	322.6	612.2	338.8	602.5	48672	0.55	6.3	301	445
20	342.6	305.6	98963	289.5	591.3	306.5	570.6	84485	3.80	24.2	538	1119
23	342.8	306.0	100440	288.0	572.7	310.1	551.6	78711	3.83	26.6	493	933
--- 80/20 Isobutane/Isopentane ---												
25A	344.0	315.1	96328	302.0	615.5	313.0	598.8	90258	2.90	18.8	528	1085
28	342.3	316.6	85599	304.7	614.8	316.6	603.0	72582	2.29	16.5	554	944
29	343.8	330.9	86270	356.6	608.2	334.7	598.5	53067	1.16	12.9	309	453
30	344.6	310.2	96560	296.2	592.8	307.0	574.4	93821	3.45	21.4	551	1193
31	344.9	316.4	96514	302.5	591.3	318.8	575.5	75087	2.86	19.4	505	989
32	342.8	324.6	85921	307.1	584.9	329.6	573.8	55691	1.64	18.9	296	426
33	344.5	307.6	100502	293.5	569.7	302.6	548.7	96419	3.85	21.9	602	1419
34	345.2	314.3	100389	298.3	568.6	316.6	550.4	77524	3.23	22.5	492	925
35	345.5	337.8	100746	324.1	565.6	338.9	550.3	57842	0.81	9.7	286	391
36	344.7	317.8	100603	304.8	619.8	315.6	602.9	85595	2.82	18.3	535	1054

Table 5

Performance for B-1 through B-5 for Selected Data Runs Using a Method Two Calculation

Test Run #	A_{dev} (%)	U	U_m	U_{dev} (%)	h_o	h_{om}	h_{dev} (%)	$LMTD_2$ (°F)	$LMTD_1$ (°F)	P_{dev} (psia)	$P-Pt_2$ (°F)	$P-Pt_1$ (°F)
Commercial Isobutane												
1	1.9	395	391	1.0	682	670	1.8	16.9	17.4	-0.7	7.9	8.3
2	5.5	388	379	2.4	651	628	3.7	17.3	18.7	-5.1	6.8	8.1
5	30.4	429	425	.9	753	746	0.9	12.8	16.7	0.6	5.5	8.5
6	18.6	422	415	1.7	751	730	2.9	14.1	16.8	0.2	7.0	9.1
7	23.3	423	424	-0.2	736	739	-0.4	14.4	17.8	-1.3	5.2	8.2
8	3.5	380	372	2.2	601	580	3.6	18.5	19.8	-6.8	2.2	2.6
10	19.4	431	429	0.5	768	761	0.9	13.6	16.4	-0.7	6.7	9.0
11	4.4	410	403	1.7	731	711	2.8	14.7	15.5	-0.3	8.6	8.5
12	12.2	414	407	1.7	727	708	2.7	15.6	17.9	-4.0	6.0	8.0
13	-5.6	300	261	14.9	509	432	17.8	15.0	16.6	-0.2	7.2	6.6
15	13.9	418	408	2.5	744	715	4.1	13.4	15.7	-2.0	6.9	8.6
Nominal 90/10 Isobutane/Isopentane												
18	34.6	394	379	4.0	671	607	10.5	14.0	19.6	0.4	4.7	8.5
19	52.8	344	330	4.2	563	529	6.4	12.3	19.5	6.4	3.4	8.1
20	113.4	421	391	7.7	741	660	12.3	8.7	20.0	-6.2	2.6	10.7
21	99.0	411	393	4.6	711	663	7.2	11.6	24.1	-8.8	2.7	11.3
22	601.7	48	322	-85.1	591	537	10.1	20.0	21.0	-15.0	-.7	8.8
23	161.8	424	394	7.6	742	662	12.1	7.1	19.9	-71.0	1.4	9.1
24	24.4	404	386	4.7	678	630	7.6	17.2	22.9	-4.7	5.9	10.5
25	38.2	336	326	3.1	554	530	4.5	13.8	19.8	-2.5	4.1	8.9
Nominal 80/20 Isobutane/Isopentane												
25A	-2.3	399	380	5.0	686	633	8.4	21.0	21.6	-0.7	10.1	11.4
26	-0.1	423	402	5.2	747	686	8.9	23.6	24.7	-3.0	12.4	13.7
28	9.0	364	391	6.7	611	551	10.9	17.3	20.1	2.0	6.8	9.4
29	57.7	366	351	4.3	601	562	6.9	10.6	17.5	14.8	2.5	7.0
30	3.8	405	380	6.6	703	535	10.7	18.8	20.7	1.0	9.4	11.2
31	22.9	397	369	7.6	668	597	11.9	14.6	19.3	2.6	5.1	8.7
32	41.8	369	348	6.0	613	560	9.5	11.7	17.6	2.5	3.0	6.8
33	4.6	415	393	5.6	723	660	9.5	17.9	19.8	-0.2	9.0	10.6
34	17.9	407	382	6.5	688	620	11.0	15.4	19.4	1.1	5.4	8.0
35	31.4	406	368	10.3	672	575	16.9	14.2	11.1	-6.6	3.7	8.2
36	11.3	410	383	7.1	696	634	9.8	17.2	20.4	0.6	7.0	10.1

Table 6

Condenser details

No. of tubes: 332
No. of passes: 1 shell side, 1 tube side[a]
Tube length: 24 ft
Tube size: 3/4 in O.D., 14 BWG.
Tube material: carbon steel (SA-214)
Tube pitch: 15/16 in., triangular array
Shell I.D.: 22 in.
Baffles: Supports

[a]Side by side

Table 7

Condenser Performance for Selected Data Scans

Test #	Time (hrs)	$r_{foul} \times 10^3$	U_m	U_{clean}	$h_{o,m}$	h_{io}	Nu	Rey_c	P_r	Q_{bal} (%)
Commercial Isobutane										
1	8.5	0.610	156	173	210	1461	.224	2480	3.6	0.08
2	10.25	0.633	151	166	202	1410	.215	1764	3.6	0.77
3	26.75	0.847	159	183	243	1005	.260	909	5.2	0.07
4	31.50	0.909	147	170	218	1055	.232	2080	4.6	1.04
5	34.75	0.951	149	173	225	1034	.240	1365	4.8	0.53
6	51.50	1.169	145	175	217	1301	.232	1936	3.8	0.67
7	53.50	1.195	141	169	208	1338	.222	2112	3.4	0.61
8*	54.75	1.211	178	227	299	1394	.319	3711	4.3	0.07
Nominal 90/10										
9	76.50	1.402	128	155	189	1274	.202	2151	3.3	0.55
10	78.50	1.419	128	157	193	1221	.206	2052	3.3	0.11
11	81.25	1.442	131	162	200	1198	.214	1625	4.3	0.17
12	98.50	1.590	126	158	201	988	.216	876	5.3	0.89
13	100.00	1.603	117	144	208	559	.222	1112	4.7	0.32
14	102.00	1.620	127	159	194	1274	.208	1881	3.3	0.28
15*	104.50	1.642	169	234	314	1346	.336	3786	4.2	0.15
Nominal 80/20										
16	149.25	2.090	114	151	182	1241	.195	2280	3.4	4.2
17	151.25	2.110	116	154	189	1181	.202	1962	4.1	4.1
18	153.25	2.130	111	145	189	809	.202	1842	4.5	3.2
19	169.75	2.295	106	140	185	728	.198	1536	4.9	4.1
20	174.50	2.343	135	198	264	1095	.286	660	5.6	1.7
21	176.50	2.363	152	237	334	1144	.360	1044	5.0	3.6
22	196.4	2.562	111	156	191	1188	.204	2244	3.7	1.3
23*	198.00	2.578	159	269	382	1335	.409	4913	4.3	5.0

*Half bundle test

SUPERCRITICAL HEAT EXCHANGE FIELD TEST (SHEFT)

TEST FACILITY SCHEMATIC DIAGRAM

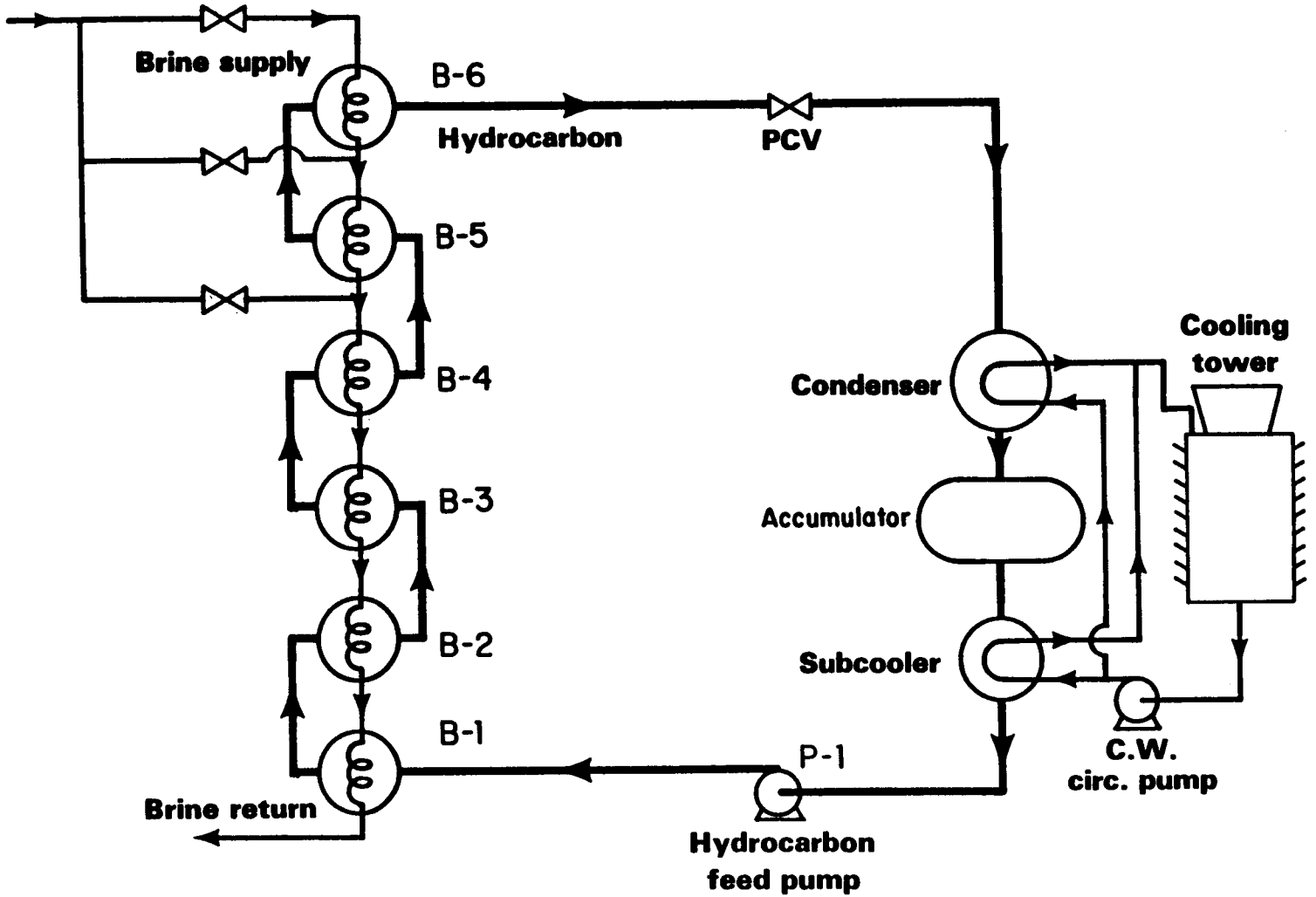

XBL 795-1420A

Fig. 1

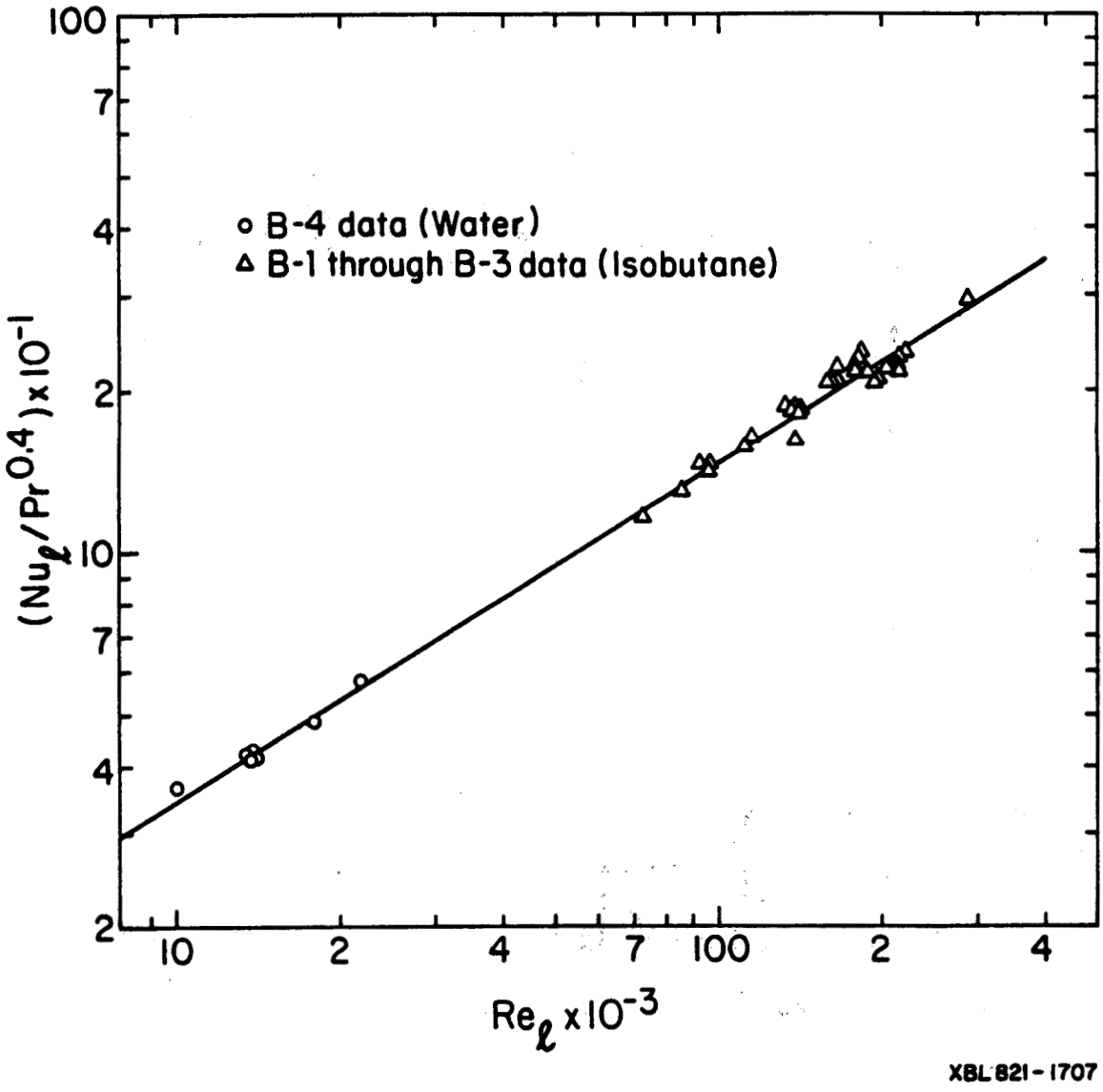

Long Flow Analysis for C_ℓ from Isobutane and Water-Water Test Data

$$Nu_\ell = C_\ell Re^{0.8} Pr^{0.4}$$

Fig. 2

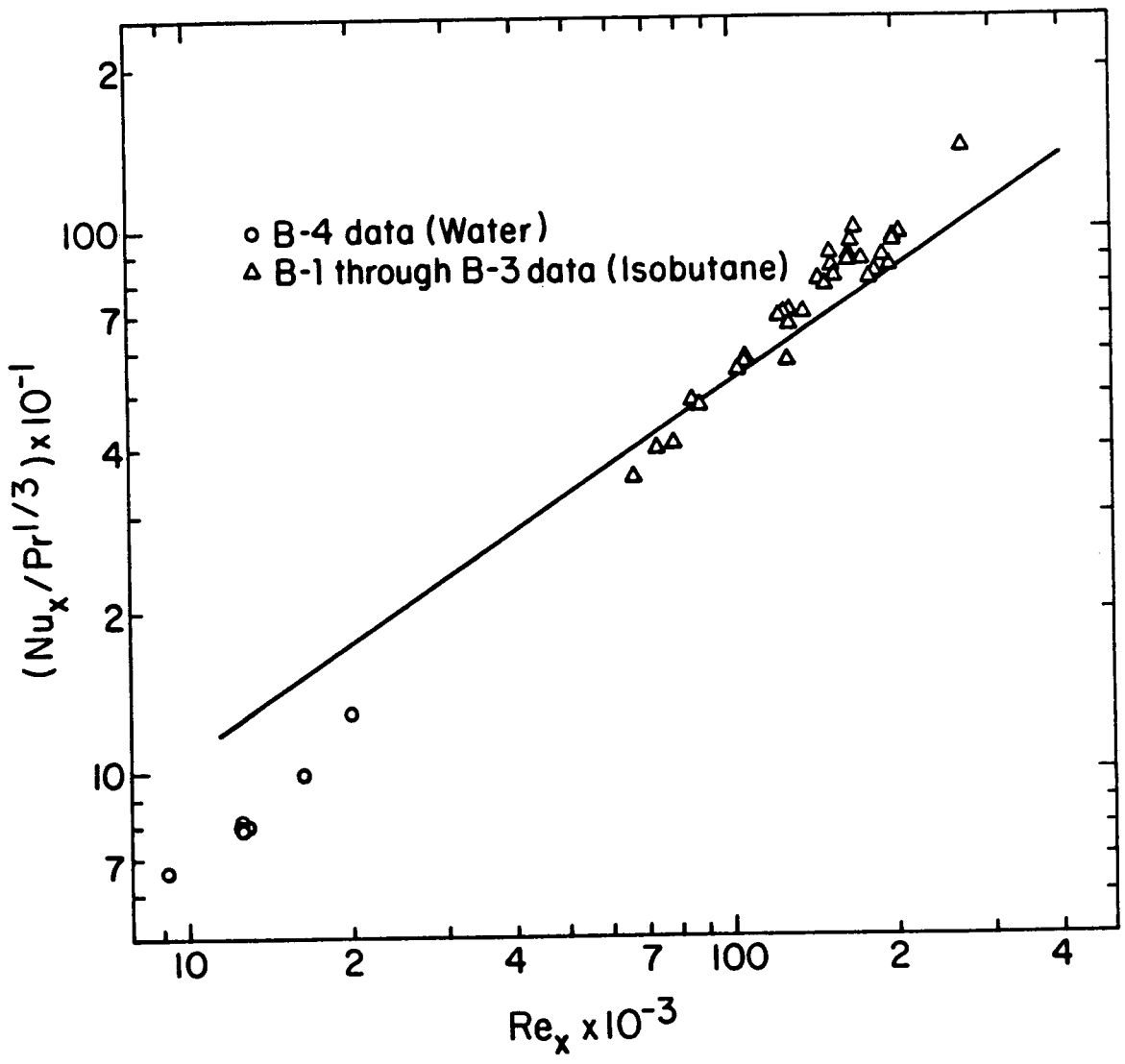

XBL 821-1708

Cross Flow Analysis for C_x from
Isobutane and Water-Water Test Data
$Nu_x = C_x Re^{0.6} Pr^{1/3}$

Fig. 3

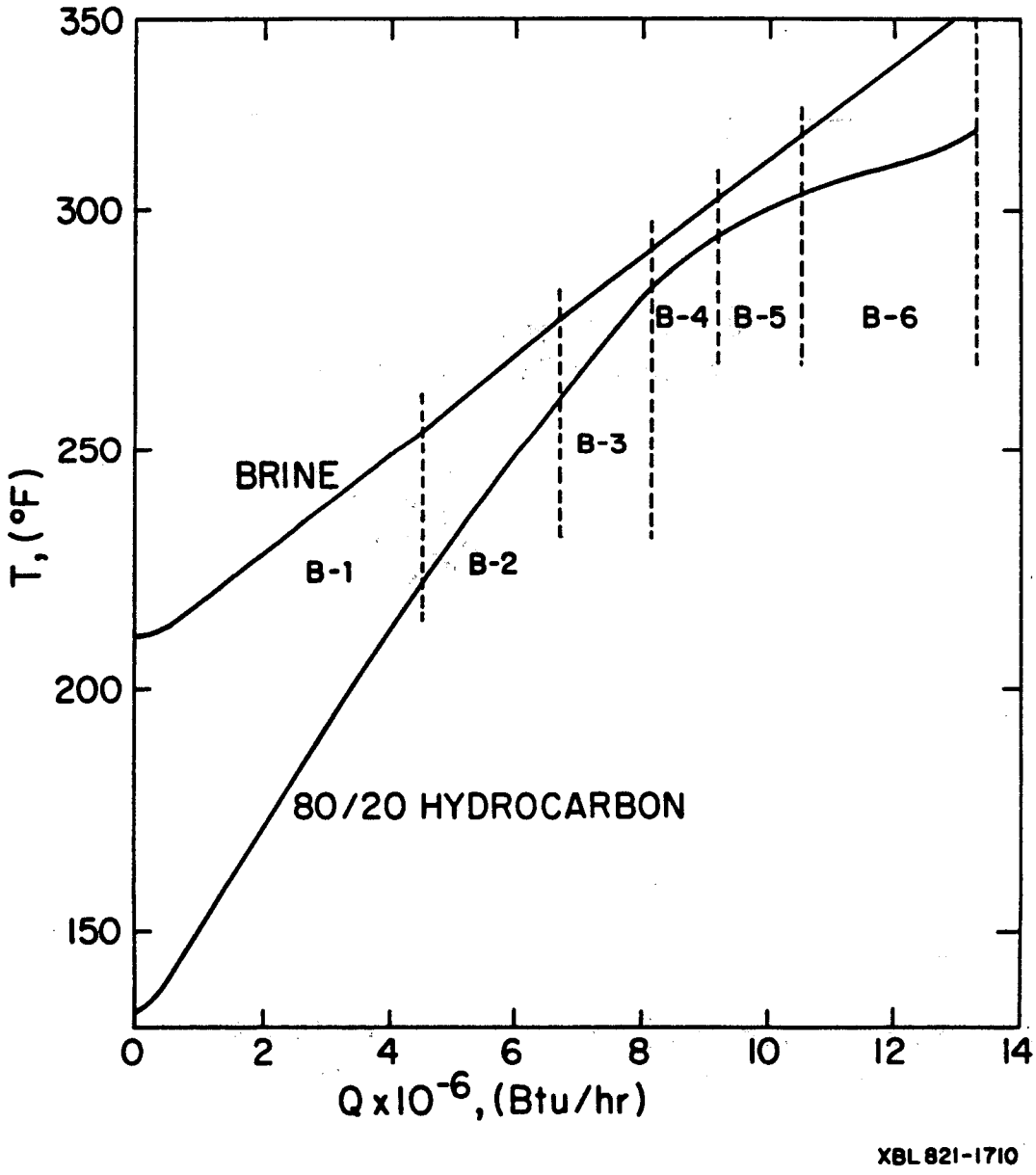

Temperature vs Duty for Nominal
80/20 Test Run

Fig. 4

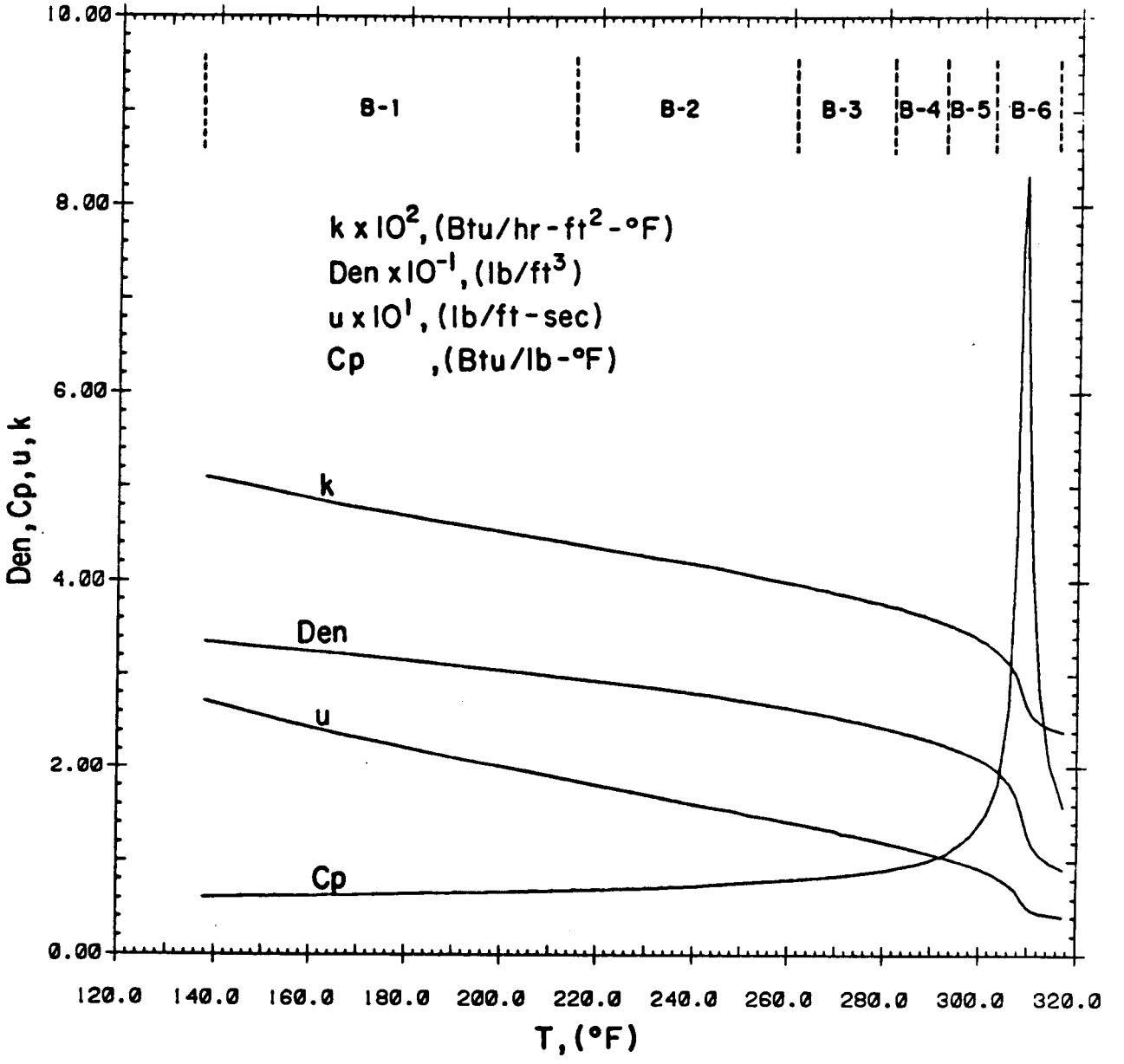

XBL 821-1732

Changes in Density, Heat Capacity, Viscosity and Thermal Conductivity for a Nominal 80/20 Test Fluid Passing through the Primary Heaters

Fig. 5

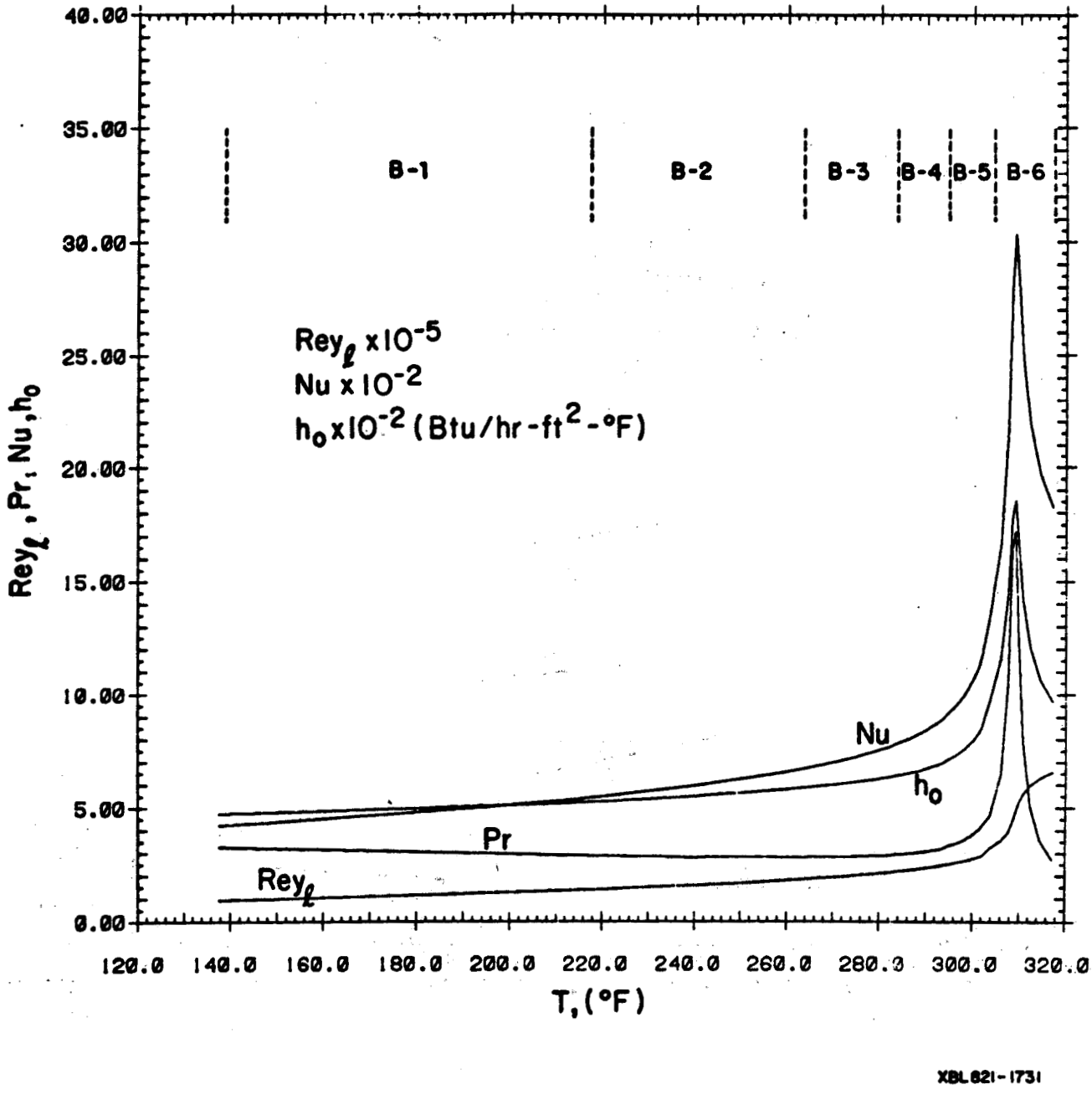

Changes in Nu, Pr, Rey$_\ell$, and h_o for a Nominal 80/20 Test Fluid Passing through the Primary Heaters

Fig. 6

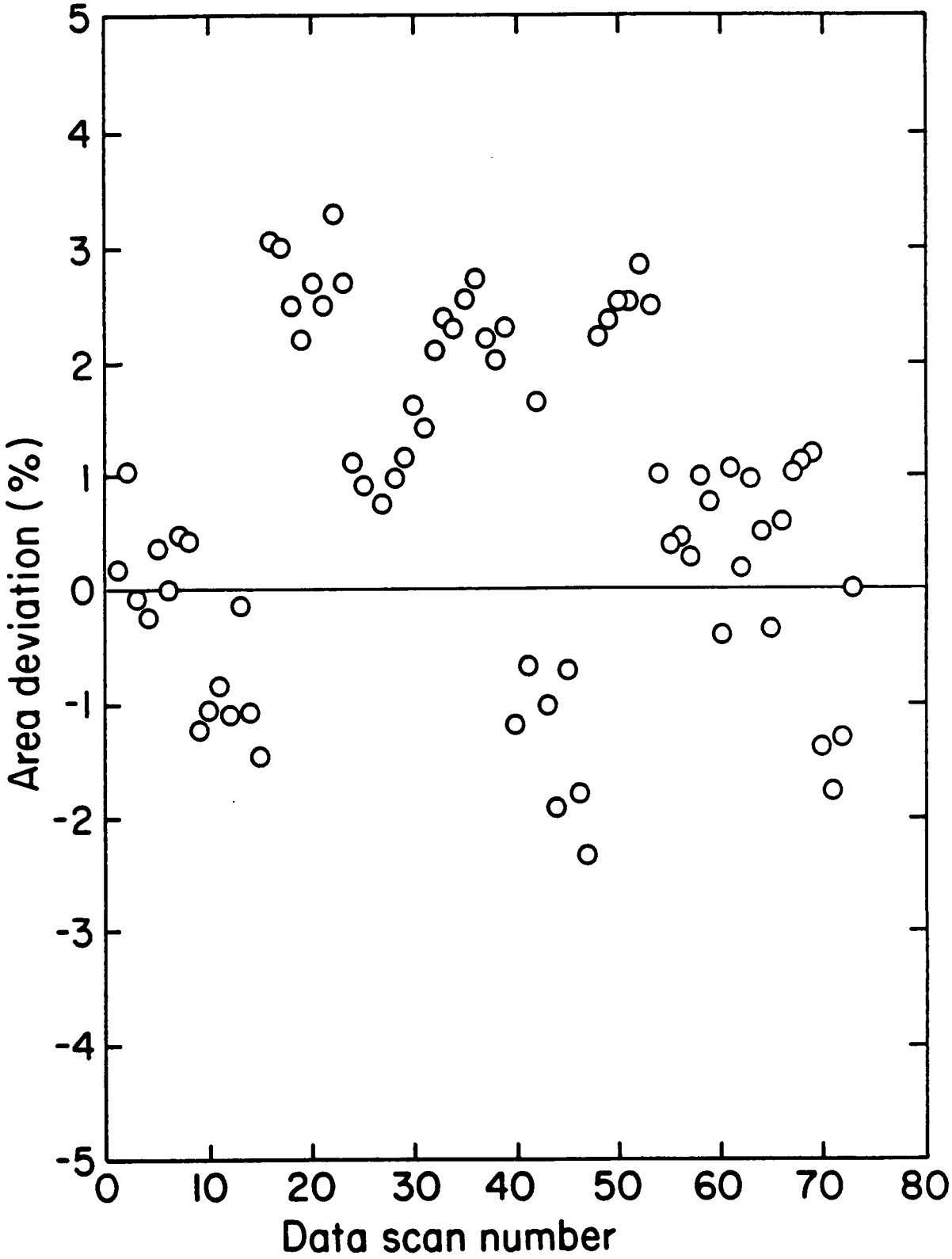

XBL 821-1713

Overall Area Deviation for Primary Heaters for
Commercial Isobutane Data

Fig. 7

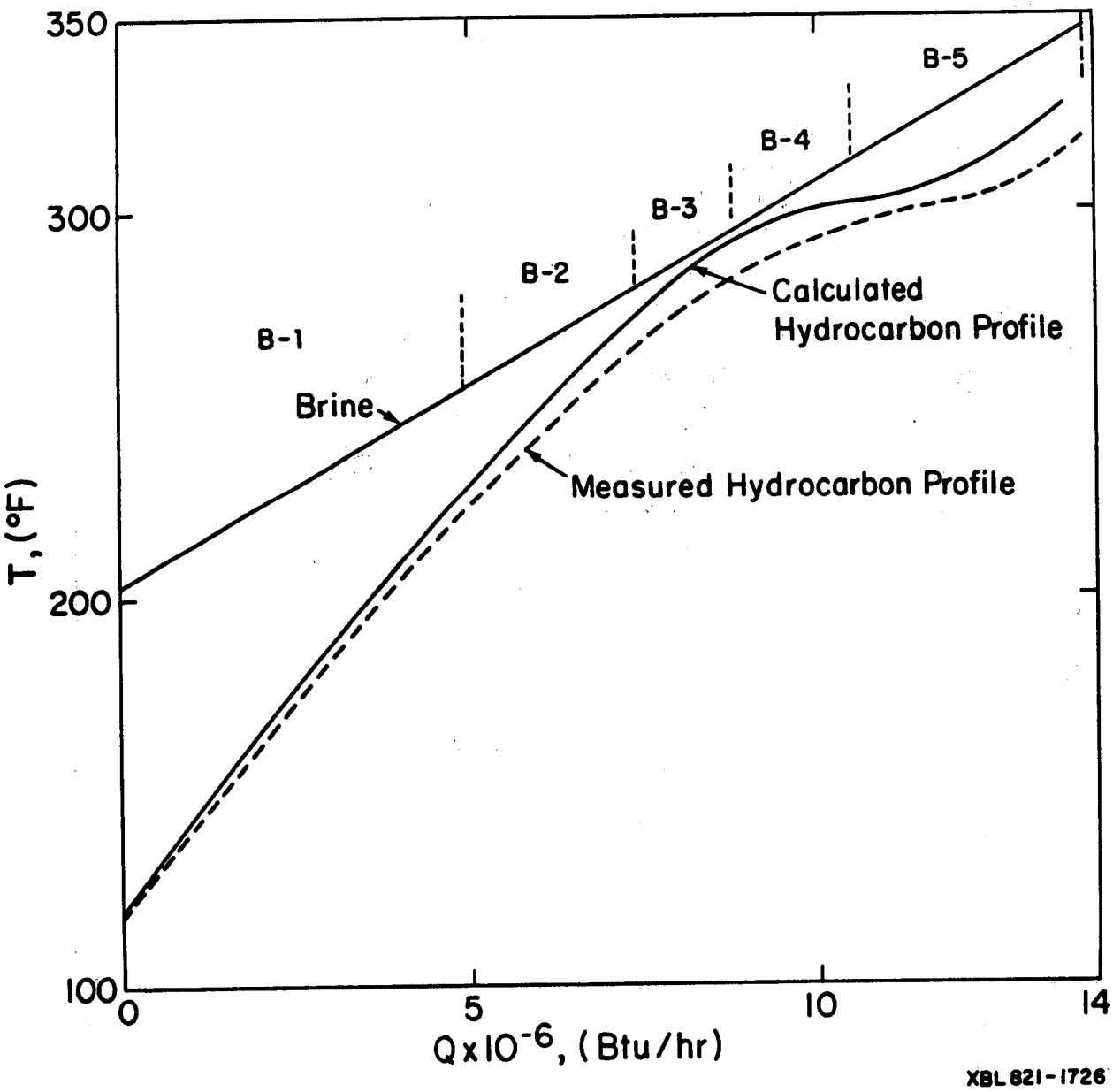

Temperature vs Duty for Nominal 90/10 Test
Fluid in Primary Heaters

Fig. 8

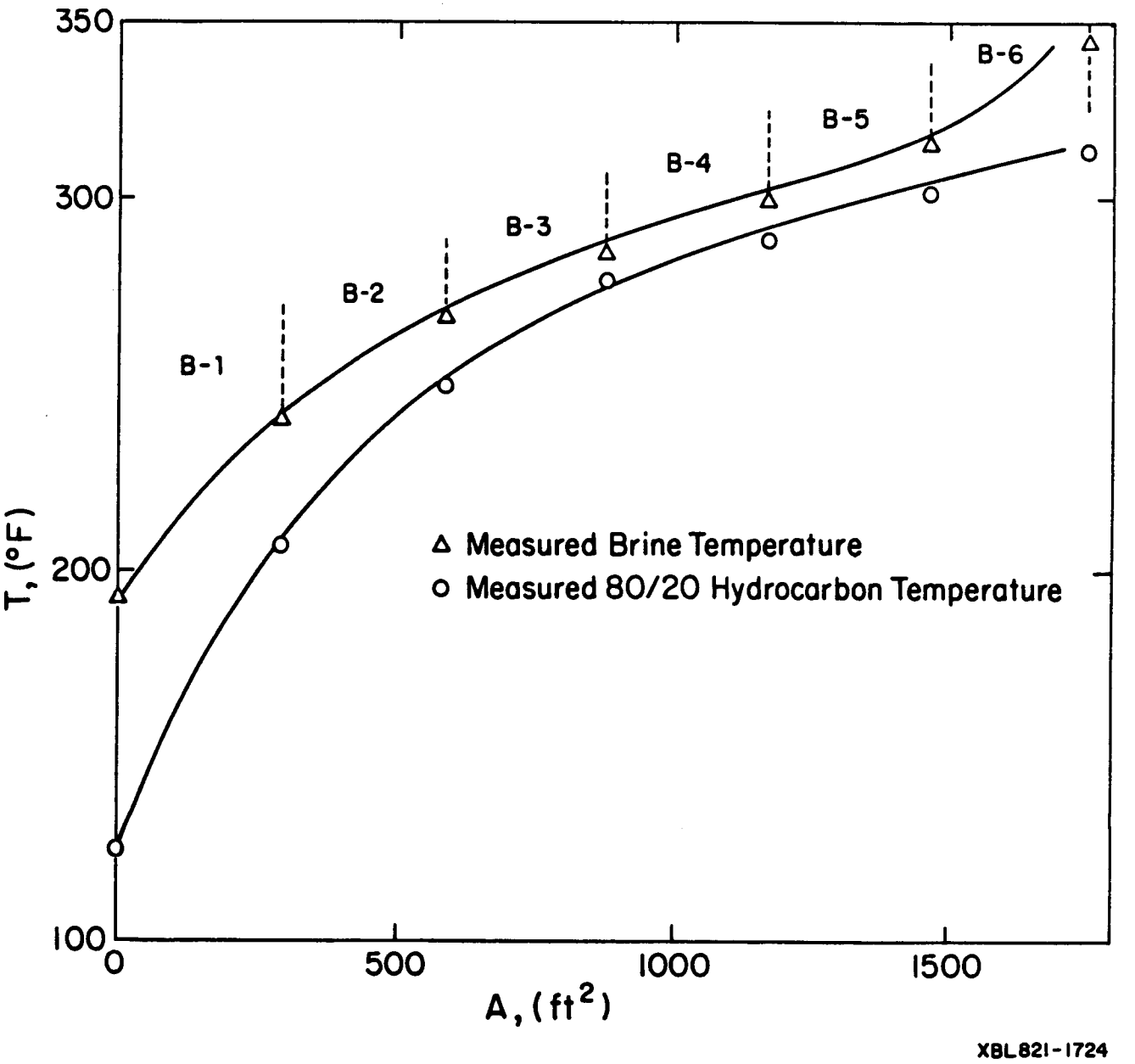

Temperature vs Area for Nominal 80/20 Test Fluid in Primary Heaters

Fig. 9

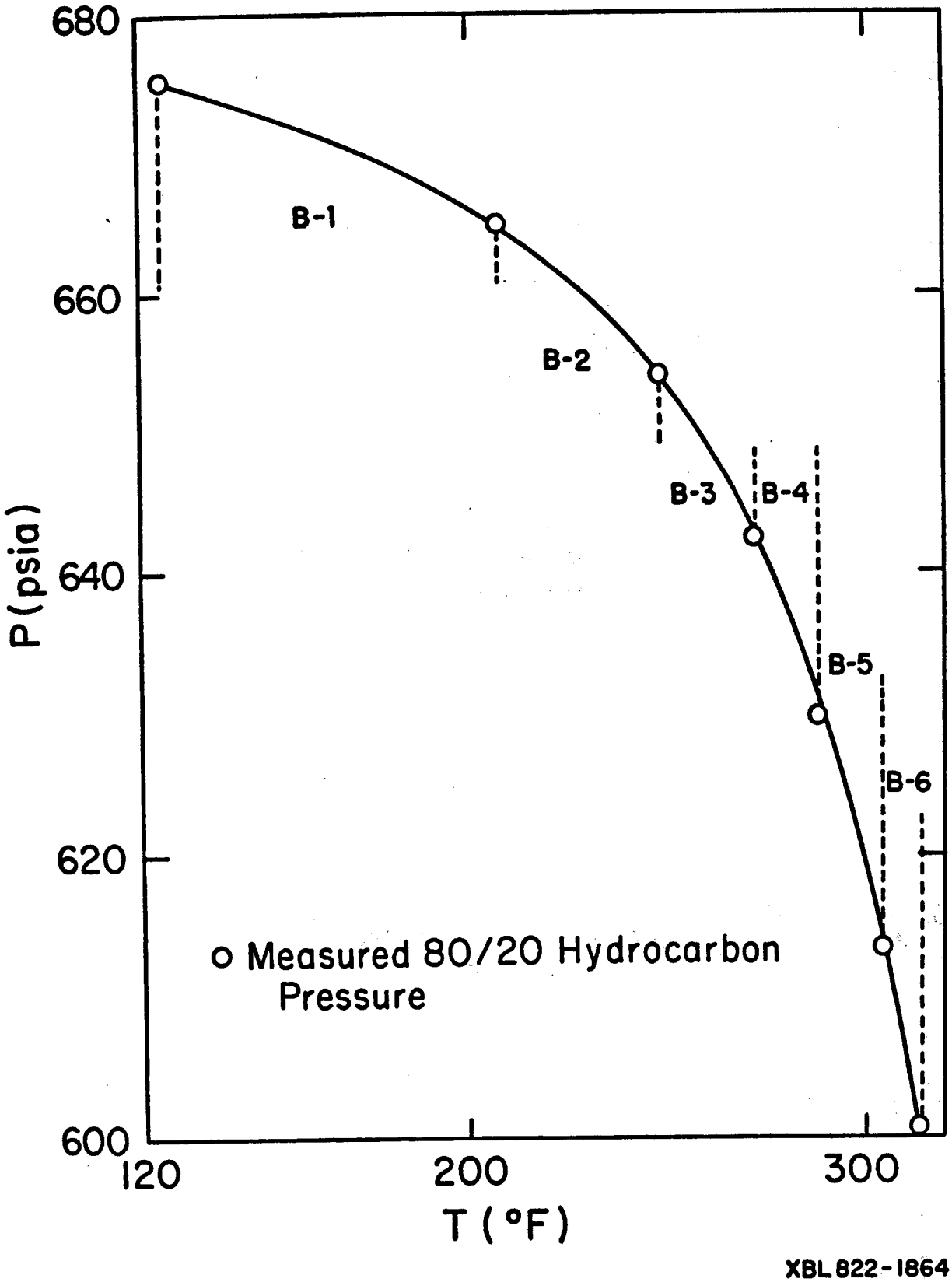

Pressure vs Temperature for Nominal 80/20 Test Fluid in Primary Heaters

Fig. 10

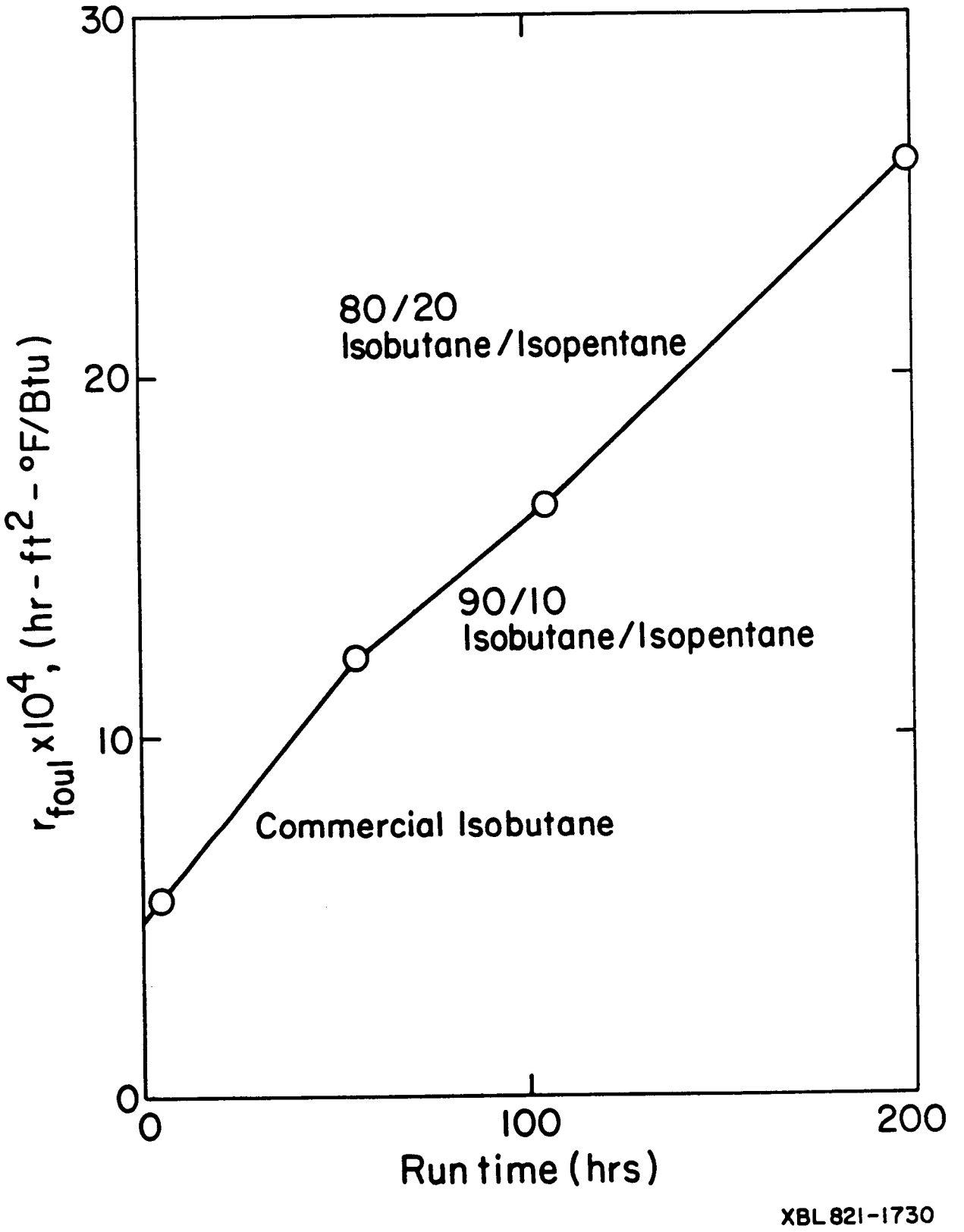

r_{foul} vs Condenser Run Time

Fig. 11

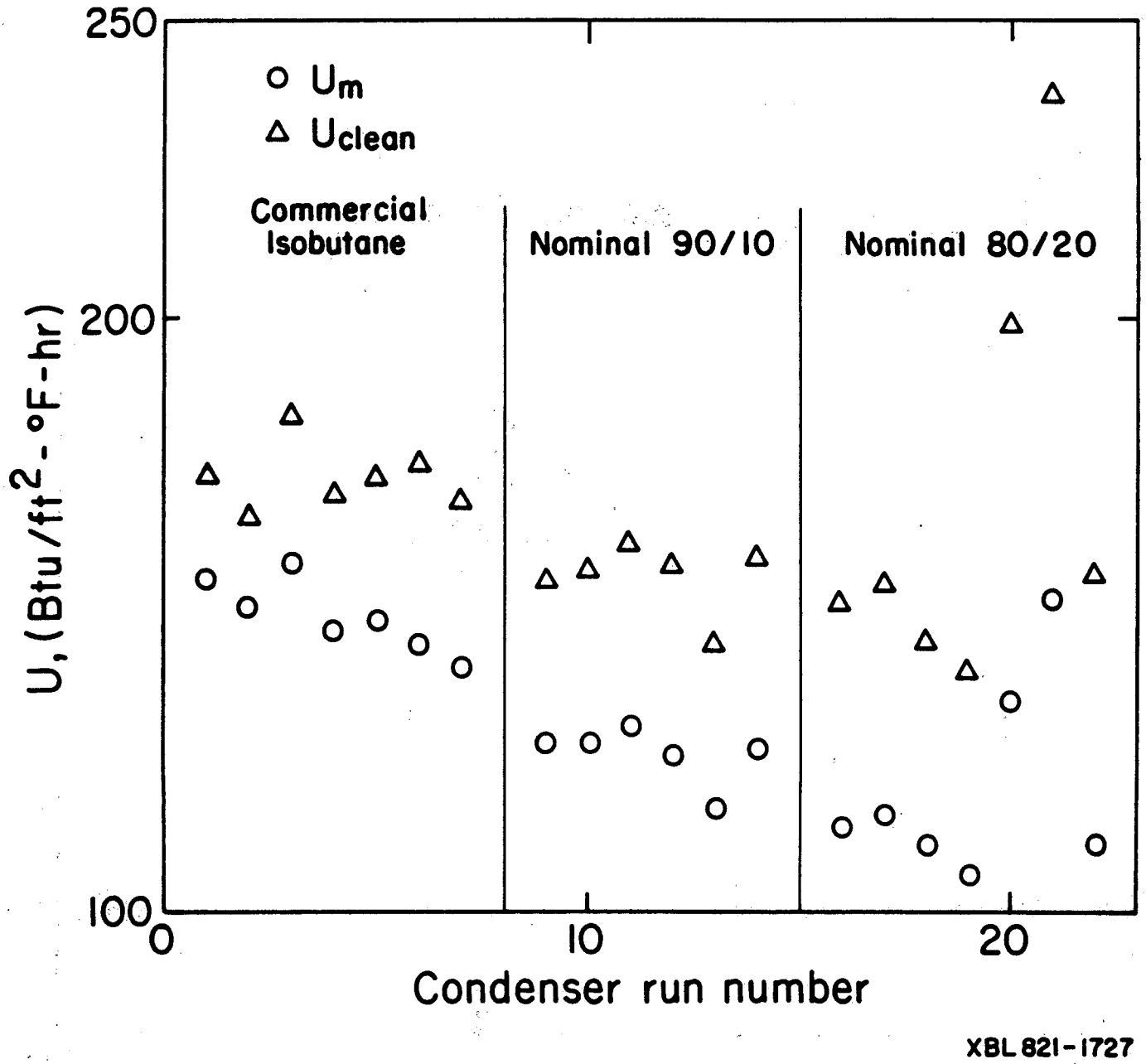

Condenser Overall Heat Transfer Coefficient vs Condenser Run Number

Fig. 12

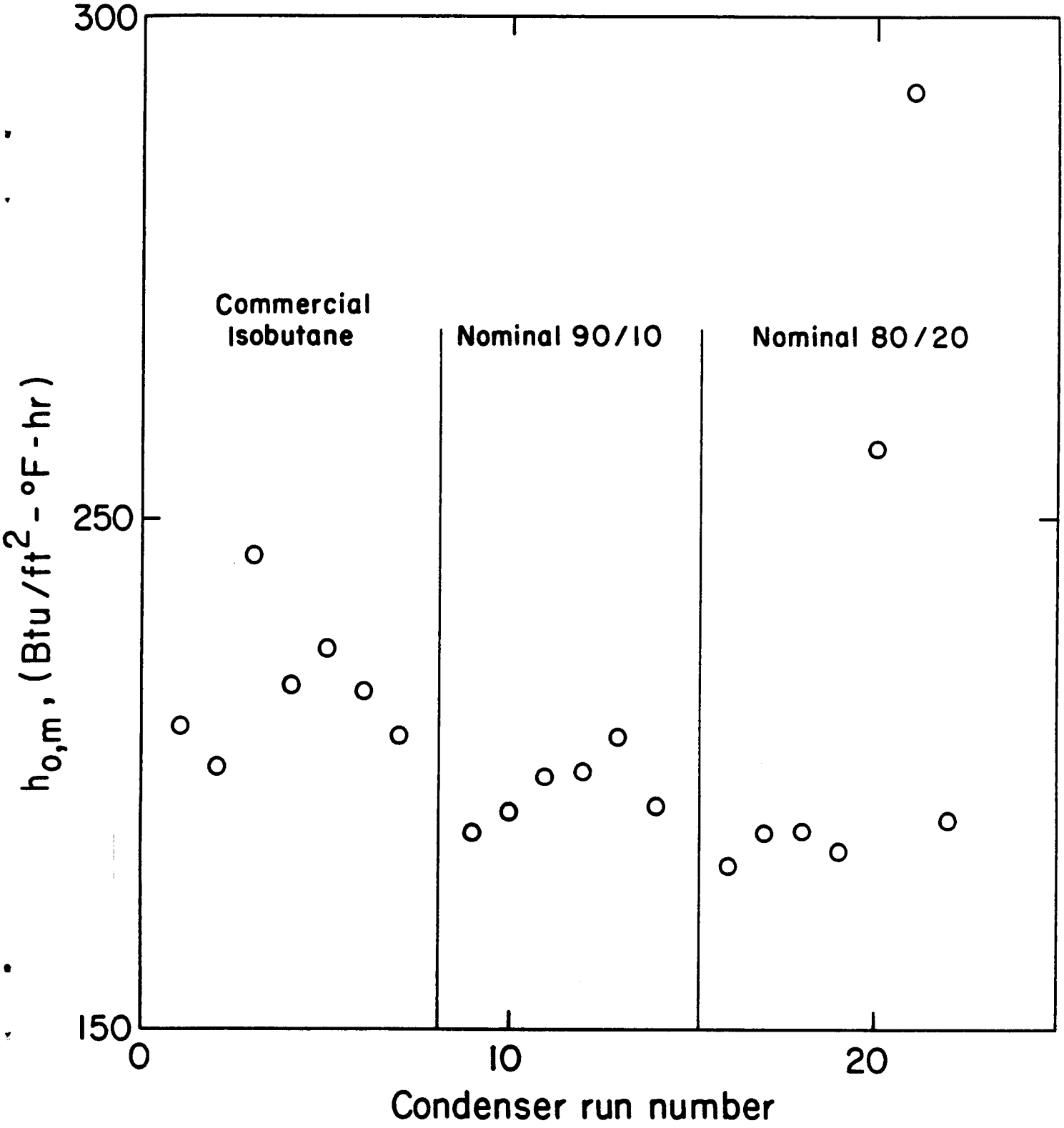

XBL 821-1728

Condensate Film Coefficient vs Condenser Run Number

Fig. 13

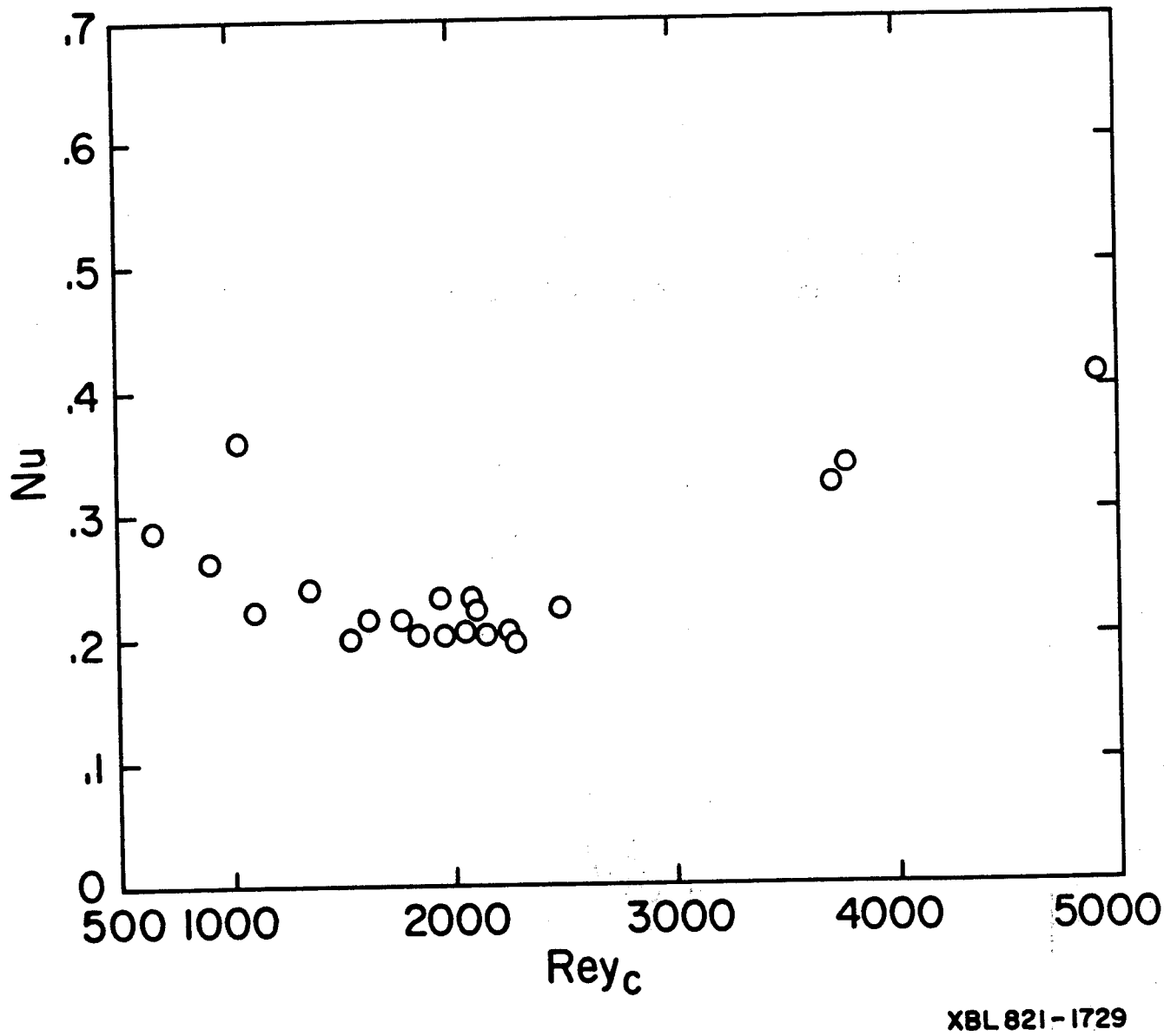

Condensate Nusselt Number vs Condensate Reynolds Number

Fig. 14